Single-Step Stereolithography of Complex Anatomical Models for Optical Flow Measurements

Diane de Zélicourt, Kerem Pekkan, Hiroumi Kitajima, David Frakes, and Ajit P. Yoganathan[1]

Cardiovascular Fluid Mechanics Laboratory, Wallace H. Coulter Department of Biomedical Engineering, Georgia Institute of Technology & Emory University School of Medicine, Room 2119 U.A. Whitaker Building, 313 Ferst Dr., Atlanta, GA 30332-0535

Transparent stereolithographic rapid prototyping (RP) technology has already demonstrated in literature to be a practical model construction tool for optical flow measurements such as digital particle image velocimetry (DPIV), laser doppler velocimetry (LDV), and flow visualization. Here, we employ recently available transparent RP resins and eliminate time-consuming casting and chemical curing steps from the traditional approach. This note details our methodology with relevant material properties and highlights its advantages. Stereolithographic model printing with our procedure is now a direct single-step process, enabling faster geometric replication of complex computational fluid dynamics (CFD) models for exact experimental validation studies. This methodology is specifically applied to the in vitro flow modeling of patient-specific total cavopulmonary connection (TCPC) morphologies. The effect of RP machining grooves, surface quality, and hydrodynamic performance measurements as compared with the smooth glass models are also quantified.
[DOI: 10.1115/1.1835367]

1 Introduction

High accuracy optical flow measurement techniques, such as LDV and PIV, require the use of transparent *in vitro* models. Complex patient-specific anatomical models have traditionally been reproduced with glass-blowing techniques, which are accompanied by high operator dependency and poor accuracy. Rapid prototyping and Computer-aided design (CAD) technology has eliminated operator dependence, enabling exact geometry replication. In literature, this approach is already described and has been applied skillfully to specific research areas of biomedical fluid mechanics [1–4]. In these studies the general methodology is to use RP with *opaque* resins to obtain an accurate water-soluble negative of the flow passage that is then encased in transparent Sylgard© (Dow Corning Inc.). This multistep process involves time-consuming chemical casting procedures and carefully controlled vacuum curing conditions. As we will describe in this Note, with the use of *transparent* RP resins these laborious casting and curing processes can be eliminated from the methodology, allowing a faster, more direct single-step transition from computer files to transparent anatomic models.

Stereolithography is being used to fabricate opaque components in wind tunnels for external flow measurements as an alternative to numerically controlled machining, Springer [5]. Chuk and Thomson [6] detail the component requirements for surface finish, dimensional accuracy, and material strength as well as production costs, time, and availability. Biomedical applications can require the analysis of large sets of small size experimental models. For most biomedical studies experimental models do not undergo important load or extreme thermal conditions. Accordingly, mechanical properties are not as crucial as manufacturing accuracy, transparency, and production time (Table 1).

In this Technical Note, our methodology is applied to the specific case of cardiovascular fluid dynamics modeling and more specifically, the total cavopulmonary connection (TCPC), which is the current surgical procedure used to repair single-ventricle congenital heart defects, de Leval et al. [7]. Two models were manufactured using transparent rapid prototyping: an anatomical TCPC connection that was reconstructed from a patient's magnetic resonance images (MRI), and an RP replica of the idealized glass model that was studied by Ensley et al. [8], both shown in Fig. 1. The later model enabled comparisons with the previous smooth glass surface experiments, and the effects of RP machining grooves on the global hydrodynamics are investigated for validation purposes.

2 Materials and Methods

2.1 Model Construction. Since the core of this method is RP, the goal is to obtain a solid computer representation of the desired model. The general procedure is to

1. Create an accurate digital model of the flow volume;
2. Invert the design within a CAD software package to obtain a solid computer model of the experimental prototype; and
3. Manufacture the experimental rapid prototype and ensure optimal optical and surface quality.

In our application the flow volume, the TCPC, is obtained from MRI. However, this methodology may be applied to other 3D imaging modalities and on any anatomical cavity. To compensate for the out-of-plane sampling limitations inherent to MRI, adaptative control grid interpolation (Frakes et al. [9]) was used to enhance the stack of raw images. The region of interest was segmented in each slice using an in-house code. The 3D representation of the TCPC was ultimately generated in MIMICS (Materialise Inc. Ann Arbor, MI), turning the smoothing on to the maximum settings, and saved as an STL file. STL files represent surfaces with triangles. Subsequently, when importing an STL representation of a volume into a CAD software package, the user obtains a large number of disjoint triangular surfaces. This problem was circumvented by converting the STL file into an IGS file within GEOMAGIC STUDIO 6 (Raindrop Geomagic Inc., Durham, NC), which warps a manifold of quadrilateral nurbs patches over the points that define the STL triangles. Using this IGS format, the reconstructed TCPC volume was imported into PRO/ENGINEER (PTC Inc, Needham, MA) design software. To assess the error introduced by the successive format changes, the blood volume used for further design operation within PRO/ENGINEER was saved as an STL and compared to the original STL file, using GEOMAGIC QUALIFY 6 (Raindrop Geomagic Inc., Durham, NC). The mean deviation was 0.02 mm with a maximum deviation of 0.05 mm.

A solid box was then designed surrounding this volume, which allowed sufficient wall thickness for mechanical strength but was maintained as thin as possible to reduce PIV light absorption (which is measured to be $\sim$15%/cm for the resin used). When possible, 4 mm proved to be a sufficient thickness for both criteria. The actual experimental model was generated by Boolean subtraction of the anatomic blood volume from the box. The main constraints for box design are to avoid image distortion and laser light scattering when performing PIV. The experiment in this scenario should be planned ahead of time to identify the axes through which the model will be illuminated and imaged. The outer surfaces facing the camera and the laser should be flat and orthogonal to the acquisition and the laser beam axis, respectively. All angles

[1]To whom correspondence should be addressed

Contributed by the Bioengineering Division for publication in the JOURNAL OF BIOMECHANICAL ENGINEERING. Manuscript received by the Bioengineering Division April 24, 2004; revision received September 13, 2004. Associate Editor: David J. Beebe.

Table 1 Comparison of transparent model alternatives. The orders of magnitude provided here are based on the cost and production time estimates that were obtained for the particular TCPC geometry shown in this study. Geometric accuracy represents the difference between the manufactured model and the corresponding TCPC geometry as it is reconstructed in Mimics (Materialise Inc., Ann Arbor, MI).

Prototype	Cost	Model complexity	Production time	Geometric accuracy	Optical qualities
Glass	Low (140 $)	Limited	Short[a] (3 to 4 hours)	Poor (2 to 3 mm)[a]	Very good
Stereolithography with Sylgard© (Dow Corning)	High[b] (550$)	Acceptable	Long (7 to 8 days)	Medium (0.1 to 0.4 mm)	Good
Direct stereolithography with no chemical process	High (455 $)	Good	Short (13 hours)	High (max 0.15 mm)	Acceptable

[a]Complexity dependent.
[b]Price including both RP and Sylgard costs.

in the box design should be away from the region of interest to avoid any light scattering within it. Depending on the geometry, these constraints may lead to uneven wall thickness, which in turn leads to uneven light distribution. The use of fluorescent particles and image postprocessing algorithms can compensate for these problems.

If the model is built as a single block, construction supports will be generated throughout the entire blood volume. Though easy to remove, these supports alter the inner surface of the model. Surface quality can be recovered with fine polishing, potentially at the cost of geometrical accuracy. However, polishing the inner surfaces of the model is not always feasible depending on dimensions and complexity. In this study, the models were split along the vessel axis into two parts. These two parts were glued back together using epoxy glue, which generated a seam. Comparative measurements demonstrated that the seam had no significant impact on data acquisition when located on the surfaces facing the laser, but would distort all the data if located on any surface facing the PIV camera. Transparent UV curable adhesives (such as Desobond™, DSM Somos®) may also be used to position components together seamlessly, but are more expensive.

While Sylgard models commonly take over a week to manufacture, our model was built in 13 h using Vantico Renshape® SL 5510 resin in a SLA 250 machine with an accuracy of 0.1 mm (0.004 in.). To preserve the optical quality of the model, no chemical curing was performed. RP models are manufactured in layers that are deposited from the bottom to the top of the prototype, as it is oriented in the SLA machine (Fig. 2). Optimal surface quality and transparency is obtained for the top surface. Our components were thus oriented so as have the inner surfaces facing the top. These surfaces underwent no further polishing or surface finish. All other surfaces were polished, first using wet sandpaper of decreasing grain size (400 followed by 600) and then using coarse and fine polishing compounds (No. 7 ''rubbing compound'' followed by No. 7 ''clearcoat polishing compound''). Any typical polishing compound could be used for this purpose. A transparent acrylic paint (Rust Oleum ''Gloss Clear 1901'') was sprayed to achieve transparency. However, slight blurring still persisted on the side surfaces. The model should thus be designed so as to allow the surfaces through which PIV images will be acquired to face the bottom of the SLA machine. Accordingly, the side surfaces will be the ones through which the model will be illuminated.

2.2 Experimental Setup. In order to test the suitability of the model for our experiments, flow visualization and DPIV were run on the anatomical TCPC model. Additionally an RP replica of the simplified glass model (Fig. 1) previously studied by Ensley et al. [8] was manufactured and the hydrodynamic power losses in both models were compared to quantify the impact of surface roughness on RP model flow.

Flow visualization was performed using an aqueous solution of

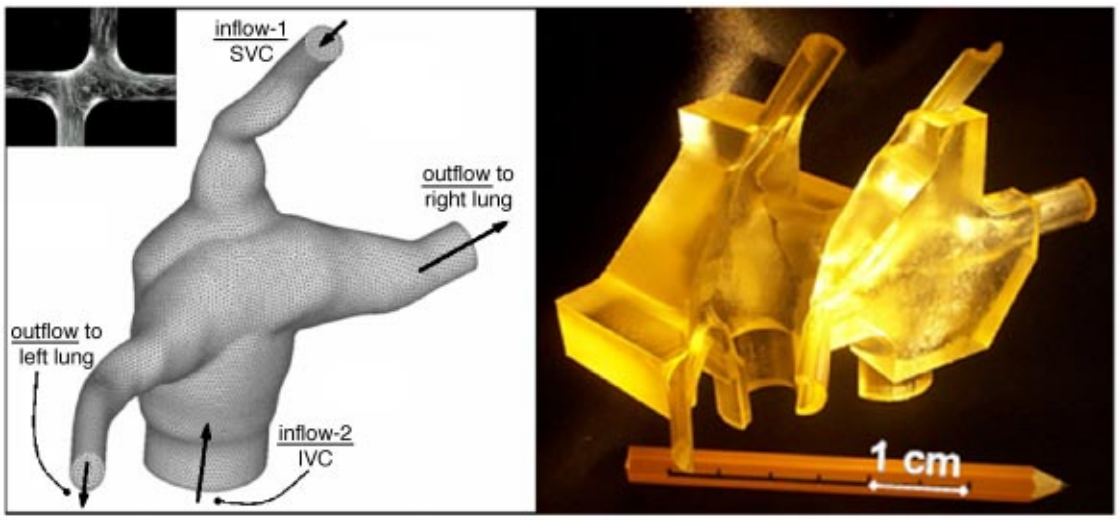

Fig. 1 Left: Unstructured computational fluid dynamics grid of the anatomic solid model, the total cavopulmonary connection (TCPC). Right: The corresponding stereolithographic duplicate for DPIV experiments, in two halves. Top-left-corner: Simple idealized planar glass model studied by Ensley et al. [8].

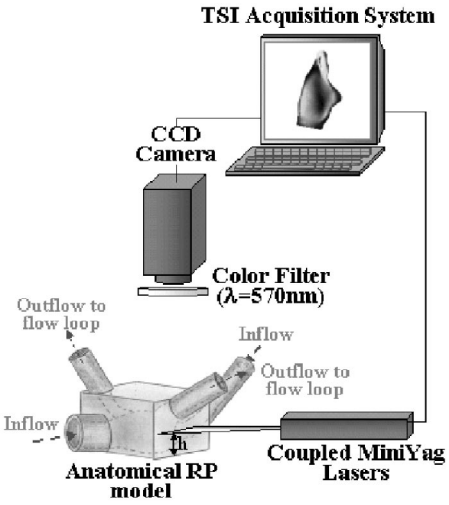

Fig. 2 Model orientation in the SLA machine as the anterior half is being manufactured and recommendations for experimental planning

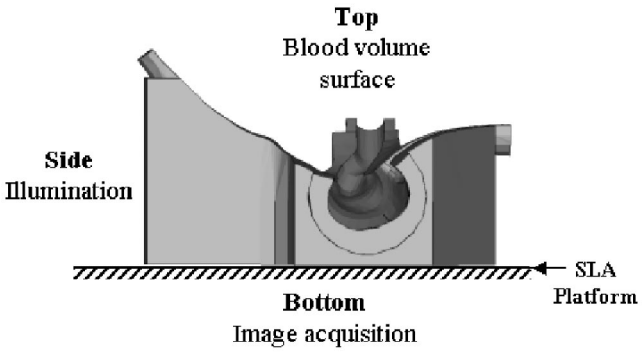

Fig. 3 PIV was performed using a TSI (TSI Inc, Shoreview, MN) system. To ensure minimum image distortion, the outer surfaces facing the camera and the laser are flat and orthogonal to the acquisition and the laser beam axis, respectively. Seeding the flow with fluorescent particles while cutting off laser light reflections with a color filter further improves PIV quality.

glycerin as a working fluid in order to match blood kinematic viscosity ($\nu = 3.5\text{cSt} + l - 0.1\text{cSt}$). A mixture of dry pigments and liquid soap was used as a dye and injected into the model by means of catheters. The model was illuminated from the posterior side with a halogen lamp. Images were acquired from the anterior side with a CCD camera at 500 frame/s, Pekkan et al. [10].

PIV was performed with a TSI (TSI Inc, Shoreview, MN) system and two 17 mJ YAG lasers (Fig. 3). The working fluid was an aqueous solution of glycerin and sodium iodide matching both blood kinematic viscosity and the refractive index of the resin ($n = 1.51$). The solution was seeded with fluorescent particles (Rhodamine-B, diameter: 2.5 to 5 μm). A color filter ($\lambda = 570$ nm) cut off all laser reflections from the model and only allowed for the light refracted from the particles to shine through. Three-hundred double-frame images were acquired at 15 Hz. An adaptive threshold algorithm was applied to the raw images to improve cross correlation. The 300 resulting velocity fields were then averaged.

3 Results

Figure 4 shows comparative results obtained in flow visualization, PIV, and CFD. Flow visualization was performed to ensure that all flow features were well captured in PIV. Two opposite inflow streams coming from the superior and inferior vena cava collided in the connection area. Due to smaller vessel diameter, the SVC flow demonstrated higher velocities than the IVC stream, and thus governed the flow recirculation in the connection area. Additionally, the curvature in the SVC at the opening of the vessel generated a flow separation region. High-frequency instability due to the two colliding inflow streams was observed in flow visualization and further demonstrated with high-order time-accurate CFD studies. The velocity fields acquired via PIV compared well with our flow visualization results and were then used to validate the CFD simulations run on the same geometry.

Hydrodynamic control volume power losses in the simplified rapid prototype (1.03, 6.30, and 18.85 mW at 2, 4, and 6 L/min, at equal lung flow split) with no inside polishing were systematically higher than those previously measured in the glass model (0.94, 5.50, 15.52 mW). These differences were not significant in the

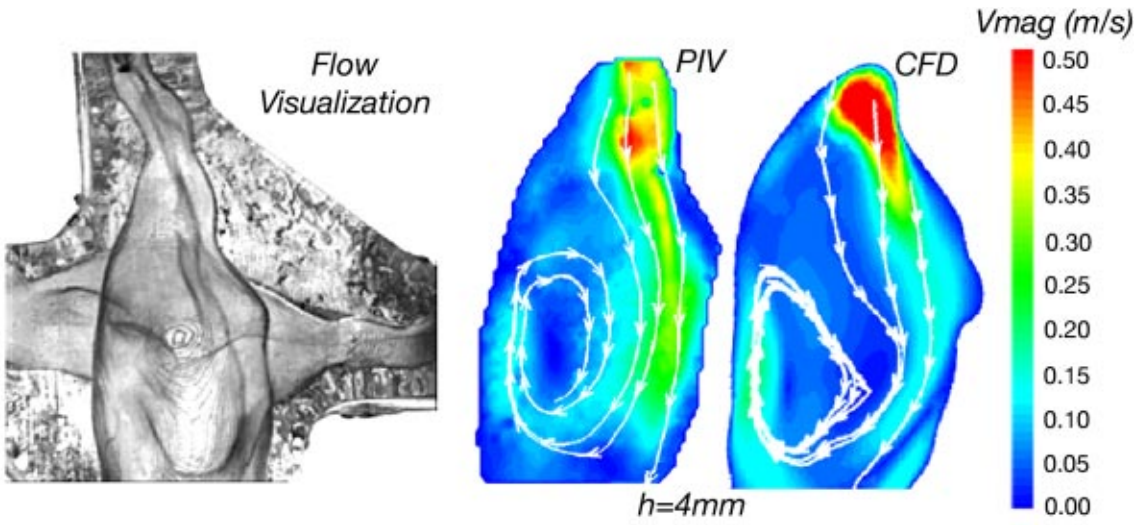

Fig. 4 Assessment of the flow field using flow visualization (left), PIV (middle), and CFD (right) at 1 L/min; inflow split: 60/40 IVC/SVC; outflow split: 30/70 left/right lung. Flow visualization dye is injected from the SVC. Height (h) is measured from model anterior. The CFD simulations were run under the same conditions and assumptions as the experimental setup, namely incompressible, laminar flow with steady inflow conditions, and rigid, but smooth vessel walls.

laminar regime ($p>0.1$ at 2 and 4 L/min, which are the normal and exercise operating cardiac outputs in Fontan children), but were at 6 L/min ($p<0.05$) where the maximum $Re_D=2023$.

4 Discussion

In this study inner model surfaces were left unpolished, in order not to accidentally alter the given lumen shape. The RP groves were shown to have no significant effect on energy losses in the laminar regime, nor to impact the PIV data for matched refractive indices. With a 0.1 mm manufacturing accuracy, the ''as is'' inner-surface roughness was measured to be 10.0 μm. It may be further reduced to 0.3 μm if polished.

The process described here is a rapid method to produce experimental models that reproduce any computer-designed geometry within a small tolerance (0.1 mm with our RP hardware) and also meet all optical requirements for flow visualization and DPIV. Specifically, anatomical configurations can be reconstructed from digitized medical images, such as MRI, and then directly converted to a solid experimental model and a CFD grid. The smoothing occurring within MIMICS cannot be exactly quantified nor completely turned off. For a better control over the accuracy of the anatomical reconstruction, an in-house code is currently under investigation.

Because it minimizes the number of steps between the computational model and the experimental prototype, this methodology is very well suited for CFD validations on complex geometries. Such an approach calls for obtaining PIV measurement in an anatomical TCPC prototype and comparing the resultant average vector fields to their numerical counterpart. With respect to cardiovascular studies, one limitation might be the model rigidity. Sylgard, as described by Yedavalli et al. [11], could provide a certain amount of compliance, like other latex- or silicone-based materials, Kerber et al. [12]. However, for real-life surgical planning or studies involving large sets of experimental models, faster model production is a critical issue. The methodology described here reduces production time from over a week to about a day, and the routine accuracy of RP machines is sufficient even for models of relatively small dimensions (on the order of millimeters). Additionally, manufacturing multiple models at the same time may further reduce the production costs. The importance of those workflow-enhancing characteristics in the context of time critical, high-volume studies cannot be overstated.

Acknowledgments

Patient data: Dr. Mark Fogel at the Children's Hospital of Philadelphia and Dr. W. James Parks at Sibley Heart Center, Egleston Children's Hospital/Emory University, Atlanta. Financial support: National Heart, Lung and Blood Institute Grant No. HL67622. Steven Sheffield, Rapid Prototyping and Manufacturing Institute, Georgia Institute of Technology, Atlanta.

References

[1] Hopkins, L. M., Kelly, J. T., Wexler, A. S., and Prasad, A. K., 2000, ''Particle Image Velocimetry Measurements in Complex Geometries,'' Exp. Fluids, **29**, pp. 91–95.

[2] Bale-Glickman, J., Selby, K., Saloner, D., and Savas, O., 2003, ''Experimental Flow Studies in Exact-replica Phantoms of Atherosclerotic Carotid Bifurcations under Steady Input Conditions,'' ASME J. Biomech. Eng., **125**, pp. 38–48.

[3] Friedman, M. H., 1993, ''Arteriosclerosis Research Using Vascular Flow Models: From 2-D Branches to Compliant Replicas,'' ASME J. Biomech. Eng., **115**, pp. 595–601.

[4] Chong, C. K., Rowe, C. S., Sivanesan, S., Rattray, A., Black, R. A., and Shortland, A. P., 1999, ''Computer Aided Design and Fabrication of Models for in vitro Studies of Vascular Fluid Dynamics,'' Proc. Inst. Mech. Eng., Part H: J. Eng. Med., **213**, pp. 1–4.

[5] Springer, A. M., 1998, ''Application of rapid prototyping methods to high-speed wind tunnel testing,'' Project 96-21, NASA Marshall Space Flight Center Technical Publication 1998-05-01.

[6] Chuk, R. N., and Thomson, V. J., 1998, ''A Comparison of Rapid Prototyping Techniques used for Wind Tunnel Model Fabrication,'' Rapid Prototyping J., **4**, pp. 185–196.

[7] de Leval, M. R., Kilner, P., Gewillig, M., and Bull, C., 1988, ''Total Cavopulmonary Connection: A Logical Alternative for Complex Fontan Operations. Experimental Studies and Early Clinical Experience,'' J. Thorac. Cardiovasc. Surg., **96**, pp. 682–695.

[8] Ensley, A., Lynch, P., Chatimavroudis, G., Lucas, C., Sharma, S., and Yoganathan, A. P., 1999, ''Toward Designing the Optimal Total Cavopulmonary Connection: An in vitro Study,'' Ann. Thorac. Surg., **68**, pp. 1384–1390.

[9] Frakes, D., Conrad, C., Healy, T., Monaco, J., Smith, M., Fogel, M., Sharma, S., and Yoganathan, A. P., 2003, ''Application of an Adaptive Control Grid Interpolation Technique to Morphological Vascular Reconstruction,'' IEEE Trans. Biomed. Eng., **50**, pp. 197–206.

[10] Pekkan, K., de Zélicourt, D. A., and Yoganathan, A. P., 2003, ''In vitro Flow Visualization of a Post-surgery Total Cavopulmonary Connection Anatomy,'' 21st Annual Gallery of Fluid Motion, APS Division of Fluid Dynamics 56th Annual Meeting, movie.

[11] Yedavalli, R. V., Loth, F., Yardimci, A., Pritchard, W. F., Oshinski, J. N., Sadler, L., Charbel, F., and Alperin, N., 2001, ''Construction of a Physical Model of the Human Carotid Artery based upon in vivo Magnetic Resonance Images,'' ASME J. Biomech. Eng., **123**, pp. 372–376.

[12] Kerber, C. W., Heilman, C. B., and Zanetti, P. H., 1989, ''Transparent Elastic Arterial Models,'' Biorheology, **26**, pp. 1041–1049.